


Modeling of pulsed electric field processing

Sudhir K. Sastry* *The Ohio State University Department of Food, Agricultural and Biological Engineering 590 Woody Hayes Drive Columbus, OH 43210, USA** Corresponding author, E-mail: sastry.2@osu.edu

Abstract

Herein, we discuss the modeling of the pulsed electric field (PEF) process, with attention focused on the originally intended application of pasteurization of liquid foods. We review literature on three classes of models. First are the models for electroporation (of molecular scale), derived from physics and physical chemistry considerations, and their extension to probabilistic approaches which treat pore formation as a random process. We discuss the more recent approaches involving molecular dynamics. Then, we consider treatment-chamber and system scale models, which are based on continuum physics approaches, and rely on computational Multiphysics codes for their solution. We then discuss the base assumptions for several modeling studies. Next, we consider models for inactivation kinetics for bacteria exposed to PEF, including the first order, Hulsheger, Peleg and Weibull models. We close with discussions of other models and experimental approaches for model verification and obtaining kinetic parameters from continuous flow PEF systems.

Citation: Sastry SK. 2023. Modeling of pulsed electric field processing. *Food Innovation and Advances* 2(3):171–183 <https://doi.org/10.48130/FIA-2023-0012>

Introduction

Pulsed Electric Field (PEF) processing in relation to foods, has its origins in the early work of Sale & Hamilton^[1,2], which recognized that electric fields could inactivate bacteria. Since that time, much research has been conducted, with a significant uptick in the 1990s, when a number of large projects were conducted with the intention of developing and commercializing PEF for pasteurization of foods. Since that time, PEF has found a niche in a variety of applications including permeabilization of eukaryotic cells.

The study of pulsed electric fields is vast and encompasses medical, environmental and food processing. Medical applications are perhaps the most advanced in that technologies are being investigated in fine-grained detail. Notably, most of the research pertains to eukaryotic cells and tissue, or in separations, and in these areas, some sophisticated modeling efforts have been conducted^[3,4].

Although the persistent theme through the recent history of PEF for food has been commercialization, it is worth considering how difficult the study of the underlying physics is, and how little progress has been made despite the availability of powerful computational tools. The purpose of this review is to investigate the work relating to mathematical modeling of PEF processes. While a number of practical applications exist, the most successful examples being for permeabilization of vegetable and cellular tissues, we focus herein on the pasteurization of liquid foods, which has received considerable attention in the literature, especially during the mid-1990s onward, when this topic was investigated in great detail. It was hoped at the time that the technology could be used for sterilization processing of low-acid, and even particulate and solid foods. While that effort has not succeeded, the pasteurization application for specific niche products has achieved commercial attention.

In the meantime, much has been written about PEF, but there still remains much confusion about the technology in the literature. Some of this is confusion regarding the fundamental distinction between sterilization and pasteurization. It is often held that PEF is a nonthermal sterilization technology^[5]. This perception is not accurate in relation to foods, as we will show in the succeeding discussion.

Sterilization in relation to foods refers to commercial sterility which implies the absence of pathogenic microorganisms that may grow in the food under normal (room-temperature) conditions of holding and distribution. If the food is low acid (pH > 4.6) this requires the inactivation of pathogenic sporeforming bacteria, especially *Clostridium botulinum*, which is highly resistant to most lethal agents. However, if the food is either acidic (pH < 4.6) or intended to be held under refrigeration following processing, the treatment is relatively mild, targeting only vegetative bacterial cells, and does not involve pathogenic sporeformers. The process may then be referred to as pasteurization^[6].

Although PEF has been shown to be effective in inactivating vegetative cells, it has not been able to nonthermally inactivate sporeforming bacteria. Only when heat is involved, does the possibility of some sporeformer inactivation become possible. Thus, PEF is not a nonthermal sterilization technology, but an effective pasteurization method.

Why model PEF? If safety of foods is to be assured, it is necessary to predict, with accuracy, whether or not the outcome of a given PEF process will result in sufficient reduction in microorganism count to safe levels. Thus, it is necessary to have quantitative relationships between populations of the target pathogenic microorganism (or its surrogate) to PEF parameters, such as field strength, waveform, pulse duration, and dead time. These are kinetics models, of which many studies exist in the literature. In addition, it is necessary to

understand the distribution of field strengths and temperatures that occur within treatment chambers during an actual process. These are the process models that require considerations of electric field, fluid flow, and heat transfer. It is the combination of these models (verified by experiment) that provides safety assurance. In addition, models can identify hot zones in treatment chambers, and indicate when there are issues of operability. There is yet another class of models; those describing cell membrane breakdown as a function of the electric field. These models form our basic understanding of PEF and attempt to describe the effect of the field on cell membranes. While not explicitly used for safety assurance, they provide the theoretical underpinnings for kinetic models.

In terms of practical applications of models, there are a number of companies currently manufacturing PEF units, including, for example, Alia, DTI, and Vitave, among others. Some of these companies are using models to determine safety as well as hot-spots and process operability^[7].

Modeling of PEF is a challenging problem as the models exist on multiple scales. At the smallest end are the molecular and cellular scales, wherein the item of interest is the cell membrane and its reaction to electric fields. While a number of modeling approaches have been attempted, detailed understanding remains an elusive goal, due not least to the small scale of investigation and the fleeting and microscopically localized nature of the changes which render experimentation difficult. Next is the treatment-chamber scale, wherein models involve computational Multiphysics approaches. This scale covers most engineering and process calculations, and although the physics is more tractable than the smaller scales, experimentation is no less difficult, due to the short timescale of the active phenomena, and difficulties in obtaining spatial resolution. Finally, kinetic models, which have been the most commonly investigated, and which are of an empirical character, for which there is a relatively large body of information.

Herein, we discuss three main classes of models: 1) molecular and cellular-scale models for electroporation; 2) continuum models for treatment chambers and their components; and 3) kinetic models for changes in food components. In addition, we summarize some kinetic model comparisons, discuss the difficulties involved in modeling PEF within continuous flow chambers, and the difficulties involved with experimental verification of the same. Finally, we discuss the difficulties involved in extracting kinetic parameters from continuous flow treatment systems.

Electroporation models

Among the early models applying physics principles to electrohydrodynamic instability was Michael & O'Neill^[8], who addressed instabilities between plane layers of fluid; their solutions were of an analytical nature, relying on stream function formulations as were common in the era before extensive computing resources. A physics-based model on bilayer lipid membranes (BLM) was reported by Crowley^[9], who modeled the BLM as an elastic capacitor, sandwiched between two layers of conducting fluid (Fig. 1).

Using a force balance between the electrical attraction forces across the membrane, and the elastic resistance offered by the insulating material, Crowley developed the relation (Eqn 1; symbols and Greek letters are explained in Supplemental File 1):

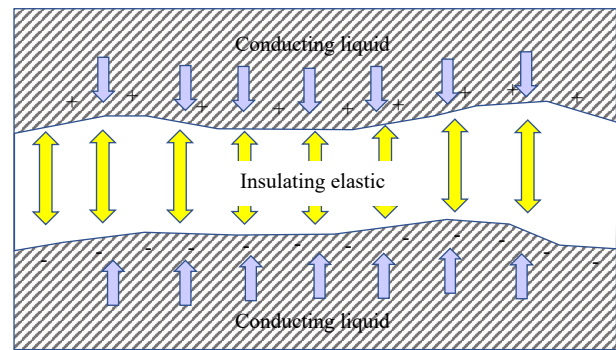


Fig. 1 Model for membrane, modeled as an insulating elastic between conducting liquid layers, after Crowley^[9]. Forces of electrical compression in blue arrows; elastic forces in yellow arrows.

$$\frac{\Delta}{L} \cong \frac{\epsilon V^2}{2EL^2} \quad (1)$$

Crowley considered a small displacement of the membrane (capacitor) from equilibrium. For a compressive displacement, the elastic force would increase, tending to return the system to its initial position; however, the electric pressure would also increase with the square of the voltage across the membrane. If electric forces dominate, the equilibrium would be considered unstable. For higher voltages, Crowley obtained the relation:

$$\frac{\epsilon V^2}{2EL^2} \cong 0.18 \quad (2)$$

This yields the criterion for instability as:

$$\frac{\epsilon V^2}{2EL^2} > \sim 0.18 \quad (3)$$

However, Crowley noted that the opposite sides of the BLM were flexible, and would deform, yielding a lower value for the voltage at which instability occurred. Also, given that bacterial cell membranes are far more complex than BLMs, it is possible that significant deviations from the theory could be observed.

Later, a detailed analysis of a BLM was conducted by Abidor et al.^[10], and Pastushenko et al.^[11]. Abidor et al. noted, using a relation of Michael & O'Neill^[8] that the breakdown voltage of a BLM would be:

$$V_* = \left(\frac{\sigma h}{\epsilon_0} \right)^{1/2} \quad (4)$$

By using values of $\sigma = 2$ erg/cm², and $h = 50$ angstroms, Abidor et al. found a value for breakdown voltage of 1 V. Although Abidor et al. considered this number to be reasonable, but an overestimate, it has become the default assumption of PEF researchers ever since.

Abidor et al. went further in developing the theory of breakdown of a BLM, by considering its physical structure in more detail than in previous work. They considered the behavior of BLM and biological membranes to be analogous and noted that the similarities could be explained by assuming that there were defects in the BLM in the form of through-going pores, which undergo random fluctuations in size, and that such pores of microscopic size could evolve to significant size resulting in macropores. They identified two distinct kinds of pores, hydrophobic and inverted, as illustrated in Fig. 2.

The thinking is that the development of such defects requires energy to create additional membrane surface, which, in the absence of an electric field is given by:

PEF modeling

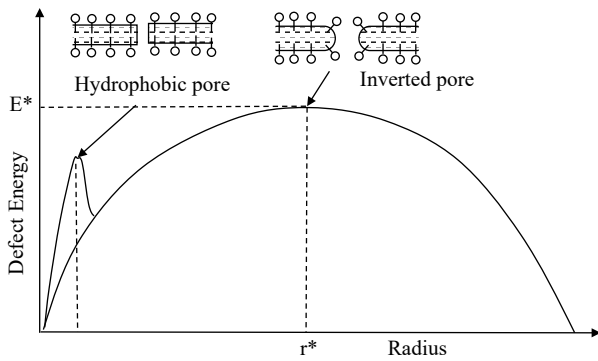


Fig. 2 Dependence of defect energy on pore radius (after Abidor et al.^[10]). The dotted-dashed peak at left shows the energy barrier required for maintenance of hydrophobic pores. Pores smaller than this energy barrier are closed, those to the right fluctuate between two energy barriers.

$$E_0 = 2\pi\gamma r - \pi\sigma r^2 \tag{5}$$

When a field is applied, the (hydrophobic) pore shown on the top left of Fig. 2 is assumed to behave as a capacitor; then the following relationship was applied:

$$E = 2\pi\gamma r - \pi\sigma r^2 - 0.5\pi CV^2 r^2 \tag{6}$$

where C is the change in specific capacitance in the region of the defect, given by:

$$C = \left(\frac{\epsilon_s}{\epsilon_m} - 1 \right) C_0 \tag{7}$$

The energy dependence on pore radius from Eqn 6 is as illustrated in Fig. 2. The maximum of the curve represents the critical radius r_* at which the system reaches the critical energy level E_* ; thus by taking derivatives with respect to r and setting the slope to zero, we have:

$$r_* = \frac{\gamma}{\sigma + 0.5CV^2} \tag{8}$$

The height of the energy barrier is then:

$$E_* = \frac{\pi\gamma^2}{\sigma + 0.5CV^2} \tag{9}$$

The Abidor theory then considers that under normal (no field) conditions, there always exist a number of defects with in any membrane, varying in size in a random manner due to thermal motion. As long as the defect size does not exceed r_* , the restoring force acts on them and the membrane remains stable. However, when r_* is exceeded, as with an electric field, the membrane expands spontaneously. According to the theory, the value of r_* depends on field strength: at very small fields, it remains mostly constant since the V^2 term in the denominator becomes small, but at high field strengths, it decreases rapidly.

Since the value of breakdown voltage of 1 V was originally developed with a number of simplifying assumptions, the above formula represents an approximation. Still, it is the conventional assumption of researchers that focus on PEF alone that high electric fields are necessary. While there is no doubt that permeabilization efficacy does indeed rise with field strength, permeabilization has been seen at field strengths in the range of 1 V/cm^[12,13].

Further development was done by Pastushenko et al.^[11] who attempted to determine the time required for a defect to rise to the critical size. Since this was considered a random process, the model used the random walk approach, resulting in a diffusion equation-type formulation for electroporation:

$$\frac{\partial c}{\partial t} = D \left(\frac{\partial^2 c}{\partial r^2} + \frac{1}{kT} \frac{\partial c}{\partial r} \frac{dE}{dr} + \frac{c}{kT} \frac{d^2 E}{dr^2} \right) \tag{10}$$

Since this work, the diffusion-based model has been the basis for most models for electroporation. Weaver & Chizmadzhev^[14], noted that implicit in the diffusion-based equation (10) is the assumption that pore population is history-dependent; so that the concept of a simple 'critical' voltage was invalid (and also confirmed by experiments).

Some of the modifications to this model have been noted by Weaver & Chizmadzhev^[14] relate to improvements on the terms involving the energy required for transport ions through the pores. These include adjustments for so-called 'spreading' resistance at the entrances of pores, which results in additional resistances to ionic movement (notably, ionic movement is strongly resisted in subcritical size pores due to the presence of a low dielectric environment within). A number of expressions have been derived for pore resistance, as well as conduction through pores using the approach of Parseghian^[15]. Notably, most of these expressions are analytical approximations based on electrical circuit theory, and do not specifically include considerations of Maxwell's equations, thus their applicability is limited.

A multi-pore modeling approach using a statistical mechanics formulation and a Monte Carlo simulation has been conducted by Shillcock & Seifert^[16]. This approach regards the membrane as a two-dimensional ideal gas of circular, noninteracting pores. The energy of a pore of radius r_j is proportional to its perimeter. The model Hamiltonian for a membrane containing N such pores is:

$$H = \sum_{j=1}^N 2\pi r_j \gamma \tag{11}$$

The partition function for the ideal pore gas is:

$$Z(T, A, \mu, \gamma) = \sum_{N=0}^{\infty} e^{\beta\mu N} \sum_{\text{states}} e^{-\beta H} \tag{12}$$

Where $\beta = 1/kT$.

The 'states' of the pore were labeled by the radii, and for identical pores, the statistical parameters for indistinguishable particles were used. The partition function for the pores was therefore:

$$Z(T, A, \mu, \gamma) = \sum_{N=0}^{\infty} e^{\beta\mu N} \sum_{\text{states}} \frac{1}{n_1! n_2! \dots n_j!} e^{-\beta\gamma \sum_{j=0}^{\infty} 2\pi r_j n_j} \tag{13}$$

From this approach, Shillcock & Seifert^[16] were able to calculate the average perimeter length $\langle L \rangle$ of all pores, and the average number of pores $\langle N \rangle$ as follows:

$$\beta\gamma \langle L \rangle = \frac{(1 + (1 + 2\pi\beta\gamma r_0)^2)}{(2\pi\beta\gamma a)^2} e^{-(2\pi\beta\gamma r_0 - \beta\mu)} \tag{14}$$

$$\langle N \rangle = \frac{1 + 2\pi\beta\gamma r_0}{(2\pi\beta\gamma a)^2} e^{-(2\pi\beta\gamma r_0 - \beta\mu)} \tag{15}$$

While this approach seems interesting in assessing the diffusive process of pores, it does not specifically incorporate electric fields in its considerations.

More recent work has focused on numerical solutions of versions of Eqn 10. Neu & Krassowska^[17] started with a modified form of the partial differential equation represented by Eqn 10:

$$\frac{\partial c}{\partial t} - D \frac{\partial}{\partial r} \left(\frac{\partial c}{\partial r} + \frac{c}{kT} \frac{\partial \phi_r}{\partial r} \right) = S(r) \tag{16}$$

where ϕ_r is a modified form of the energy of the defect, modified from the pore energy E to account for the presence of a transmembrane potential V :

$$\phi(r, t) = E(r) - \pi a_p V^2 r^2 \quad (17)$$

where:

$$a_p = \frac{1}{2h} (\kappa_w - \kappa_m) \epsilon_0 \quad (18)$$

and $S(r)$ is a source term to account for creation and destruction of pores:

$$S(r) = v_c h \frac{1}{kT} \frac{dU}{dr} e^{U/kT} - v_d c H(r_* - r) \quad (19)$$

where $H(r_* - r)$ is the Heaviside step function, reflecting the fact that only pores with $r < r_*$ are being destroyed; and:

$$U(r, t) = u(r) - a_p V^2 r^2 \quad (20)$$

The equation was transformed to a more tractable ordinary differential equation by defining the pore density $N(t)$ as:

$$N(t) = \int_0^\infty c(r, t) dr \quad (21)$$

which now yields a solely time-dependent function $N(t)$ which is determined by asymptotic approximation. Essentially, this reduces the calculation to a kinetics-based approach.

The asymptotic approach of Neu & Krassowska^[17] has been used, together with a Mesh Transport Network Method (MTNM) by Smith^[18] for modeling electroporation of cells and tissue in two dimensions. The primary simplification used was that the pores were assumed not to expand, and that pore creation proceeded much more rapidly than pore expansion, an assumption said to be more appropriate for very large electric fields. The space between the nodes of the mesh were modeled as equivalent electrical circuits. The use of extremely short pulses were seen to produce 'supra-electroporation', in which minimum (0.8 nm) pores form in all membranes. This was stated to be in contrast to existing hypotheses that such short pulses would not allow time for charging, while allowing smaller molecules and organelles to react. A number of results were obtained, which await independent experimental confirmation.

A separate (and more rigorous) approach has been the use of molecular dynamics (MD) simulations to understand pore formation at the atomic level^[19,20]. A more recent set of simulations^[21], which has been verified quantitatively against experimental describes a MD model for the BLM that shows the stages of pore formation. This simulation results show the formation of a membrane-spanning water file, which then progresses through the stages to final pore formation.

One of the key conclusions is that the dynamics of formation of a single prepore is verifiable both by simulation and separately conducted experiments^[22], and contradicts the relation based on capacitance change given earlier by Abidor et al. in Eqs 6 & 7.

In summary, the understanding of the pore formation process by electric fields has proven to be a daunting exercise, since the molecular scale size of membranes challenge the ability of continuum mechanics codes in simulation. However, enhanced capabilities in molecular dynamics offer the opportunity for much further development.

An attempt has been made^[23] to model the electric field distribution in the vicinity of a yeast cell and a bacterial cells of two shapes. For this purpose, they used the continuum-based

equation for the electric field:

$$\nabla \cdot \sigma \nabla V + \frac{\partial}{\partial t} [\nabla \cdot \epsilon \nabla V] = 0 \quad (22)$$

The vicinity of the microorganisms was meshed and solved using finite element simulation, with different properties identified for the food matrix, cell walls, membranes and cytoplasm. The electric field distribution was found to be maximum at the poles (aligned with the field) and a minimum at the equators (perpendicular to the field). A notable feature of this model was the incorporation of a time-dependent electric field.

Treatment chamber scale: continuum mechanics models

Models of PEF processing for foods typically focus on the scale of treatment chambers wherein a flowing (typically liquid) food material is subjected to electric pulses. At this scale, models are more amenable to the tools of continuum mechanics, and typically, computational multiphysics approaches are used.

An example of a commonly used design of treatment chamber is the co-field chamber^[24] (sometimes referred to as collinear) design illustrated in Fig. 3.

The typical governing equations for these models are:

Electric field:

$$\nabla \cdot \mathbf{J}_i + \frac{\partial \rho_i}{\partial t} = 0 \quad (23)$$

Where the total current density, \mathbf{J} is the sum of individual currents \mathbf{J}_i over i species. In the absence of convective flow, the \mathbf{J}_i s are given by:

$$\mathbf{J}_i = \sigma_i \mathbf{E} - D_i \nabla \rho_i \quad (24)$$

$$\nabla \cdot \mathbf{E} = \frac{\rho}{\epsilon} \quad (25)$$

A realistic solution to the transient relations above requires the knowledge of the species present in the system, together with their concentrations, diffusivities and electrical conductivities. This is often beyond current knowledge bases, thus many modeling approaches use the simpler steady-state Laplace equation formulation, and considering only the total (rather than species-wise contributions to current. This may be obtained by summing Eqn 23 over all species i and assuming steady-state, thus the time derivative goes to zero. This recasts this relation as:

$$\nabla \cdot \mathbf{J} = 0 \quad (26)$$

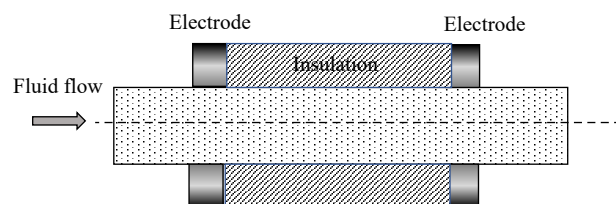


Fig. 3 Schematic diagram of a section of a co-field (also called collinear) PEF treatment chamber. The electric field here is in line with the flow, designed to restrict current through liquid foods of high electrical conductivity. A PEF unit may consist of many similar treatment chambers in series. The geometry may also vary, to restrict hot zones in the electric field, while maintaining the same fundamental concept.

PEF modeling

Then, substituting Ohm's law from Eqn 24 (after summing over all species and neglecting diffusive contributions), the familiar Laplace relation is obtained:

$$\nabla \cdot \sigma E = 0 \tag{27}$$

Since:

$$E = \nabla V \tag{28}$$

Eqn (27) can be stated as:

$$\nabla \cdot \sigma \nabla V = 0 \tag{29}$$

which is the familiar form used in most work.

A notable point about PEF models is the need to identify two distinct periods: when the field is on, and when the field is off. The consideration of this transient is important to this simulation, since the heating at the hot spots of treatment chambers can be underestimated without it. Further, the time necessary to adequately cool the hot zones are dictated by the dead time (interpulse duration), thus the determination of the optimal duty cycle is dependent on accurate models.

Although it is possible, in principle, to operate PEF in batch mode, it has been found that bacterial inactivation was more rapid in continuous flow^[25], hence subsequent designs of treatment chambers have focused on continuous flow designs. In such modeling studies, it is normal to use an electric field equation, such as Eqn 23 above, although in practice, the Laplace equation (Eqn 27) is in more common use.

Various works have been conducted^[26–30] that have considered the electric field only, and not the flow.

Transport equations

The rest of the equations are those associated with heat, mass and momentum transport as follows:

Continuity equation for fluid medium (assumed incompressible):

$$\sum_{i=1}^3 \frac{\partial v_i}{\partial x_i} = 0 \tag{30}$$

where v_i is velocity in the i th coordinate direction.

Fluid momentum equations (one each for each direction j):

$$\rho \left(\frac{\partial v_j}{\partial t} + \sum_{i=1}^3 v_i \frac{\partial v_j}{\partial x_i} \right) = - \sum_{i=1}^3 \frac{\partial \tau_{ij}}{\partial x_i} - \frac{\partial p}{\partial x_j} + B_j \text{ for } j = 1, 2, 3 \tag{31}$$

Energy equation (with viscous dissipation assumed negligible):

$$\rho C \frac{\partial T}{\partial t} + \rho C \sum_{i=1}^3 v_i \frac{\partial T}{\partial x_i} = \sum_{i=1}^3 \frac{\partial}{\partial x_i} \left(k \frac{\partial T}{\partial x_i} \right) + u''' \tag{32}$$

where u''' is the internal energy generation given by:

$$u''' = |E|^2 \sigma \tag{33}$$

Species equation:

$$\frac{DC_n}{Dt} = \frac{\partial C_n}{\partial t} + \sum_{i=1}^3 v_i \frac{\partial C_n}{\partial x_i} = \sum_{k=1}^3 \frac{\partial}{\partial x_k} \left(D_n \frac{\partial C_n}{\partial x_k} \right) + R_k \tag{34}$$

In general, these same relations are used in computational multiphysics codes to solve for field strength, fluid pressure, velocities, and temperature. The species equation may be used for determination of component concentrations or the inactivation rates of target microorganisms.

An important component of modeling PEF processes is to recognize that there are two distinct situations that occur periodically. Firstly, when the field is on (typically on the order of microseconds), the internal energy generation term u''' given by Eqn 33 must be included in calculations. However, once the pulse is completed, $u''' = 0$, and an entirely different

calculation process must be considered. Often, this interpulse duration (field off, or dead time) is significantly longer than the pulse, and serves as the period in which heat is dissipated, and its end provides the initial condition for the next pulse. Depending on the hot and cold spots during the previous periods, the outcome of the next pulse may be quite different from the first; this would continue until a steady periodic condition is achieved.

A number of solutions have been published in the literature. Fiala et al.^[31] modeled a system with the electric field in line with the flow referred to as a co-field (also sometimes called collinear) system, by coupling the electric field, continuity, momentum and energy equations. One key assumption was that the heat generation due to the time-varying electric field could be approximated to a steady-state value by applying a factor of $f_{rep}\tau$, to the energy generation term to account for the fraction of time that the field was on. While this is a useful approximation when attempting to determine the average level of reaction (or inactivation of microorganisms) that are distributed through the chamber, it does merit reexamination, since electric fields at electrode ends can typically be very strong, and result in intense local heating in areas where flow velocities are low. Indeed, Fiala et al.^[31] cautioned that this assumption was best suited for situations where the product experienced a large number of pulses in its passage through the treatment chamber (i.e. dead time is a small fraction of residence time).

Subsequently, a series of studies have modeled the PEF process in continuous flow chambers; these include a review^[32], addressing inactivation of *E. coli* and milk alkaline phosphatase^[33]; modeling PEF on a pilot scale^[34], and studying the cooling of electrodes^[35]. Each of these studies have used the same assumption as Fiala et al.^[31] despite Fiala's conditions not being satisfied. Another study considers static PEF chambers, and solves the electric field equation (Eqn 27) and thermal conduction equation (Eqn 32 without the convective velocity terms) to predict electric field strength and temperature within the chamber, assuming no convection^[36]. They determine reaction kinetics from microbial survivor data. It is difficult to determine from the paper whether or not separate periods for field on and field off were considered.

The consequence of Fiala's assumption is that the energy generation is treated as a volumetric rate that is spread out and diffused over the entire process time. Since electric fields in PEF processing are very strong, and energy generation is proportional to the square of field strength, such assumptions may greatly underestimate the extent of local heating occurring within treatment chambers. While this may not be of much consequence for certain products and applications, due to turbulent mixing, (microorganisms of concern being at the fastest-moving centerline and far away from hot spots), or insensitivity of ingredients to temperature, the operability of the process for high-protein products that are prone to fouling and arcing may be underpredicted. This point has been made by Delgado et al.^[37] who discuss various modeling approaches for novel thermal and nonthermal processing of foods. They comment on the limited number of modeling studies; and also specifically comment on the need to minimize field heterogeneity within treatment chambers to minimize nonuniformity of treatment or to prevent dielectric breakdown due to field intensity peaks. Delgado et al.^[37] also caution that nonuniform

distributions can be caused either by electrode design or by product impurities such as air bubbles and fat globules that can cause dielectric breakdowns in the region of intense fields. This is a caution against models that violate the Fiala assumption and average the heat generation to result in underpredicted peak intensity fields. A continuous flow co-field (aka collinear) system has been modeled by Salengke et al.^[38], which does not use the Fiala assumption, and treats the pulsing and dead-time periods as separate entities. When pulsing occurred, Salengke et al. solved the electric field equation (Eqn 29), continuity (Eqn 30), momentum (Eqn 31), and energy (Eqn 32) equations, while using Eqn 33 for the energy generation term. During the dead time (interpulse duration), they did not solve the electric field equation, but solved the continuity (Eqn 30), momentum (Eqn 31) and energy (Eqn 32) equations, with the internal energy generation rate in the energy equation being set to zero.

Salengke et al.^[38], studied three different treatment chamber designs, under both laminar and turbulent flow conditions. Example results for the temperature distribution at the end of each pulse are shown (for three designs) in Fig. 4 (laminar flow in (a) and turbulent flow in (b)).

As may be seen from these simulation results, the temperature at the electrode edges at the end of each pulse approaches a high value (500° K for Design 1, assuming the system is pressurized sufficiently to prevent evaporation); although it may be mitigated somewhat by treatment chamber design (405° K for Design 2, and 330° K for Design 3). Turbulent flow was much more effective in reducing overheating, showing a maximum temperature of 343°K for Design 1, 315° K for Design 2, and 310° K for Design 3.

During the dead time (interpulse duration: in this case, 2 ms), some cooling occurs at the electrode edges, as shown in Fig. 5 ((a) for laminar and (b) for turbulent flow) for all three designs. Example temperatures at the electrode edges from Salengke's work (not previously published) shows the progression of temperatures during successive pulses, as indicated in Fig. 6.

The results from such transient simulations can be useful in optimizing field strength, pulse and interpulse duration, as well

as chamber design to avoid overheating and maintain stable operation. The simulation in Fig. 6 represents a turbulent flow situation, and shows a stable progression of maximum temperatures at the hottest edge, indicating that the interpulse duration is sufficient for cooling and stable operation in this case.

Relatively few other efforts have involved modeling of PEF systems. Pataro et al.^[39,40] have modeled the electrochemical phenomena at the electrode-solution interface of PEF systems. Their approach involves the solution of the Nernst-Planck equation:

$$\frac{\partial C_n}{\partial t} = \sum_{i=1}^3 \frac{\partial}{\partial x_i} (N_{ni}) + R_n \quad (35)$$

where:

$$N_{ni} = - \left(D_n \frac{\partial C_n}{\partial x_i} \right) - z_n u_{m,n} F C_n \frac{\partial \phi_n}{\partial x_i} + C_n v_i \quad (36)$$

The calculation of the velocities, v_i were calculated from the equations of motion, together with the energy equation, as detailed earlier in Eqns 30 - 32. The boundary conditions involved detailed expressions for the Faradaic current densities and the charge accumulation at the electric double-layer at the electrode-solution interface.

In conducting these simulations, Pataro et al.^[40] described the details of simulations over the duration of several pulses to quantify the migration of metal ions into solution. The model described experimental data well for Trizma HCl buffer, but showed some deviations for Mclvaine buffer.

Other computational models have been developed^[41,42]. The possibility of optimization of the entire temperature history through the process has been noted^[43] (although the work is for High Pressure processing, the same principle could apply to PEF).

Jaeger et al.^[44] developed a model that enabled the quantification of thermal and electric field effects during PEF inactivation of alkaline phosphatase (ALP) and lactoperoxidase (LPO) in milk, as well as *Escherichia coli* in apple juice. The flow and heat transfer problems through the entire system were solved using FLUENT. Their work suggests that heat was the major component of inactivation.

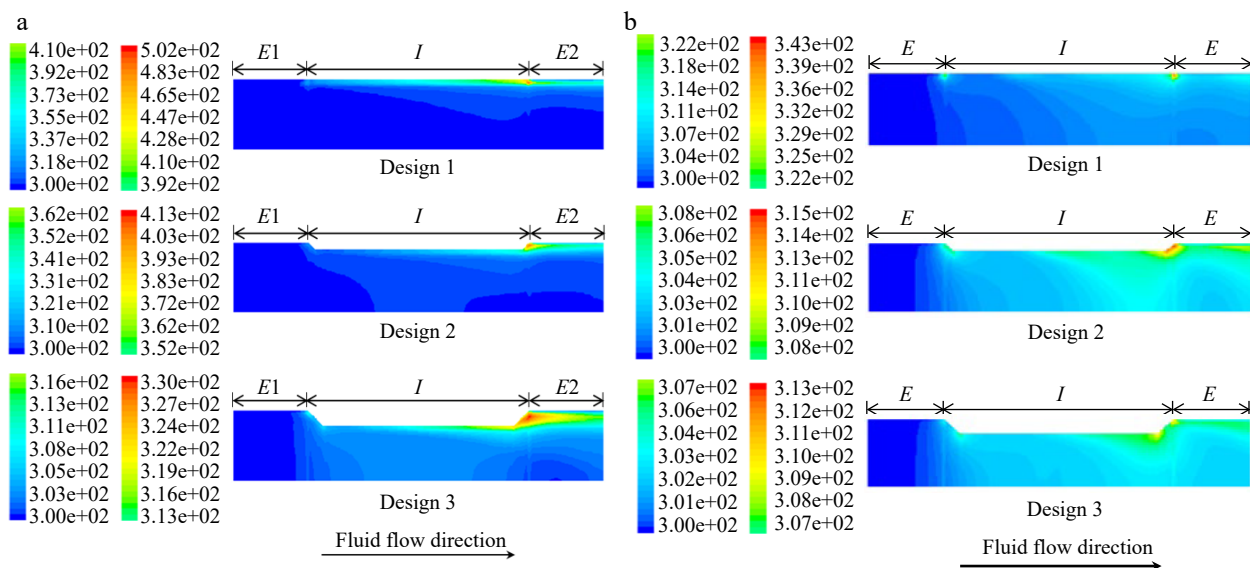


Fig. 4 (a) Temperature profiles in a co-field (aka collinear) PEF treatment chamber at the end of a 1.4 μs pulse of 60 kV under (a) laminar flow, and (b) turbulent flow. From Salengke et al.^[38].

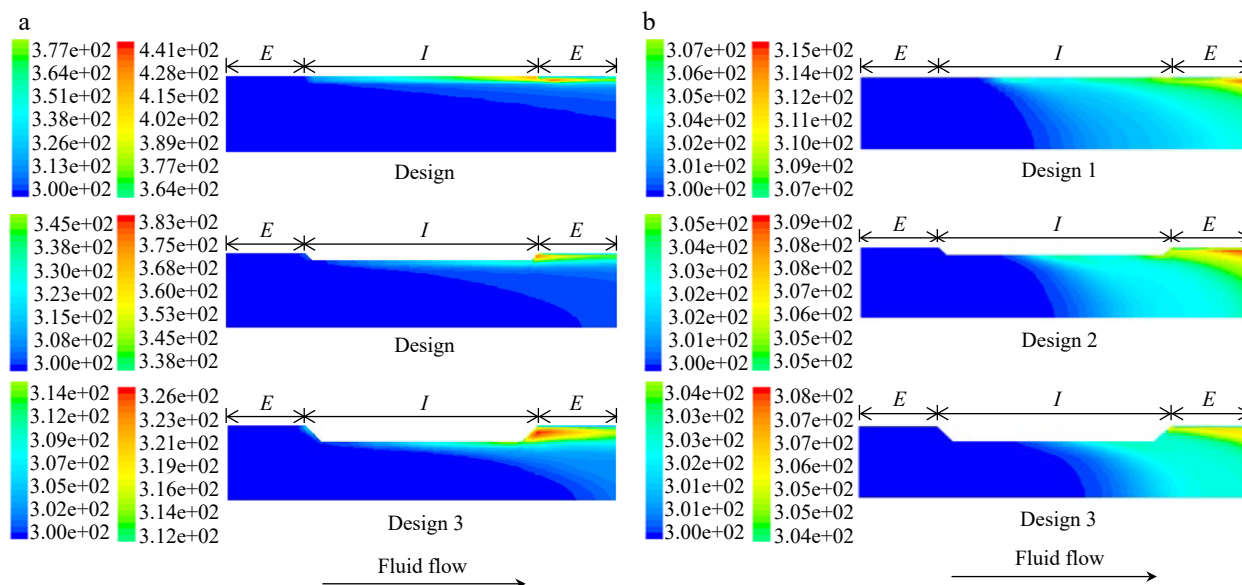


Fig. 5 (a) Temperature profiles in a co-field (aka collinear) PEF treatment chamber at the end of a 2 ms interpulse duration following a 1.4 μ s pulse of 60 kV under (a) laminar flow, and (b) turbulent flow. From Salengke et al.^[38].

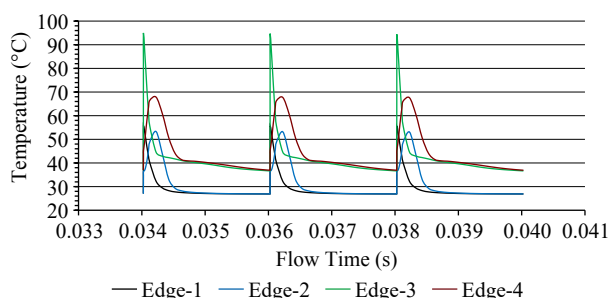


Fig. 6 Temperature histories at various electrode edges of a treatment chamber, as simulated by Salengke et al.^[38] but not previously published. Edge 1 represents the most upstream location of the upstream edge, Edge 2 is the downstream location of the upstream edge, Edge 3 is the upstream location of the downstream edge, and Edge 4 is the downstream location of the downstream edge.

Buckow et al.^[45] compared lactoperoxidase inactivation during PEF processing with that using heat, and concluded that much of the inactivation in a co-field (collinear) PEF system was due to thermal reasons, while a small portion ($\sim 12\%$) of the inactivation was not attributable to temperature effects alone. In this sense, the work agrees with Jaeger et al.^[44].

Duvoisin et al.^[46] describe a system for treatment of foods within packages during continuous flow, and describe a model for the same. The model uses the equations of Ganea^[47] involving ozone discharge, which are essentially circuit versions of the Poisson equation (Eqn 25), thereby treating the problem as one of electrostatics. No time-dependent terms were described.

Difficulties in experimental methods

There are two major difficulties involved in measurements to support PEF modeling efforts: those involving experiments for measurement of reaction kinetics in flowing systems, and those involving verification of process models in such systems. We

will deal herein with the issues involving verification of process models. The difficulties in determination of kinetics will be covered in the next section on kinetic models.

Difficulties in verification of process models

In-situ measurements within PEF systems are, in general, extremely difficult, due to the fleeting nature of pulses. While the indirect consequences of the field (heating) might be measured using imaging techniques, direct *in-situ* measurement of electric field distribution during PEF is not currently possible. The other major challenge is the measurement of temperature distribution within the PEF chamber.

Some attempts have been made to measure variables such as temperature within flowing PEF systems^[34] using a fiber-optic probe inserted into the treatment zone, or thermocouples in treatment chambers. However, it should be noted that such measurements may not only disturb the flow, but the sensors are unable to respond quickly to the changes in the electric field and the resulting sharp changes in local temperature. For example, fast fiber-optic sensors may have a response time of 10 ms (or $10^4 \mu$ s); for a PEF treatment involving 5 μ s pulses at 600 Hz, this means that six pulses would have elapsed before the sensor even begins to register a measurement. For the moment, there is not an option outside of modeling. However, these require the transient approach of Salengke et al.^[38] rather than steady-state approaches.

In connection with a static system, Saldaña et al.^[36] measured temperature within a microbial suspension (assumed to be a solid matrix) while avoiding the pitfall of disturbing the field with the sensor. This was done by a specially designed cell^[48] wherein the sensor was inserted into the PEF chamber using a pneumatic activator after pulsing was completed. This approach enables a measurement of temperature immediately following pulsation, but does not attempt to make an *in-situ* transient measurement within an electric field. This approach is useful for determining the thermal consequences of one or more pulses following treatment.

Kinetic models

The purpose of kinetic models is to enable the design of processes to ensure adequate pasteurization (or sterilization, for low-acid foods, although this is not relevant to the PEF case). Towards this end, a number of models have been examined. In general, kinetics models are largely of empirical origin, and their parameters are typically obtained by curve-fitting of experimental data. Some models (e.g. Weibull) do have some basis in probabilistic approaches, but still rely on curve-fitting. Thus, while useful in specific situations of process design, and for specific pathogen-product-process combinations, they are not universally applicable. Herein we consider a few models that have received attention in the literature.

First-order models

These are historically the most common models used in the literature, and have been the basis of thermal process designs. These have the form^[49]:

$$\ln(Y) = \frac{2.303t}{D} \tag{37}$$

where:

$$Y = \frac{N_t}{N_0} \tag{38}$$

A related model in this context is that used by Sensoy et al.^[50] which includes a critical treatment time t_c .

$$\ln(Y) = \frac{t - t_c}{k_t} \tag{39}$$

where the form remains the same as Eqn 37 except for having time starting from the critical treatment time (t_c) which refers to the minimum treatment time for inactivation to occur. This is determined from the inactivation curve being extrapolated back to 100% survival (referred to as a shouldering effect). However, for *Salmonella dublin*, Sensoy et al.^[50] found that in all cases t_c was zero.

Although this has been a commonly used approach originating in the thermal processing literature, it has been noted that many data sets from the literature, while fitted to straight lines on a log scale, actually do show various deviations from linearity^[51]. In more recent times, data from nonthermal processes have shown pronounced shouldering and tailing. Thus, current approaches include consideration of models that account for these deviations.

Hulsheger model

From Hulsheger et al.^[52] and studied further by others^[49,50]:

$$Y = \left(\frac{t}{t_c}\right)^{-(E-E_c)/k_c} \tag{40}$$

where:

$$t = n\tau = nRC \tag{41}$$

The critical electric field strength (E_c) is calculated from relations such as that of Eqn 4, or from the relations given by Sale & Hamilton^[53] or Weaver & Chizmadzhev^[14]. As mentioned earlier, these relations have been developed with numerous simplifying assumptions and may not apply in many situations.

Since the Hulsheger equation relies on numerous assumptions, its usefulness may be limited. One is the assumption of a typical RC circuit time constant, which was appropriate for their system involving discharge of a capacitor (exponential decay waveform), but may not apply in this form to pulses of different

waveforms (although it is possible to use pulse duration as a substitute for square-wave pulses). Further, the electroporation relations on which the critical field strength is based are themselves based on simplifying assumptions. Thus the relation needs to be used with caution. San Martin et al.^[54] have found that the Hulsheger model was not adequate for describing their experimental data. Huang et al.^[49] present a detailed discussion of the model's applicability and tests of its efficacy.

Peleg (Fermi) model

Peleg^[55] proposed a model based on Fermi's equation, previously used for biomaterials, and repurposed it for PEF applications as:

$$Y = \frac{1}{1 + e^{(E-E_c(n))/k_c(n)}} \tag{42}$$

where the critical field strength E_c and kinetic constant k_c both depend on the number of pulses, n , which also implies a time-dependency for each of these parameters. These values have been modeled by Peleg as:

$$E_c = E_{c0}e^{-k_1n} \tag{43}$$

$$k_c = k_{c0}e^{-k_2n} \tag{44}$$

Sensoy et al.^[50] have recast the above equations in terms of time, as:

$$E_c = E_{c0}e^{-k'_1t} \tag{45}$$

$$k_c = k_{c0}e^{-k'_2t} \tag{46}$$

Peleg's model has been used to successfully fit the inactivation rates of several microorganisms^[50,54,56]. The value of E_c has been seen to decrease with the number of pulses, although an increase of E_c has been found at the largest numbers of pulses^[54].

Weibull model

The Weibull model has been widely used in a number of nonthermal processing applications. The version we discuss here is based on that of Mafart et al.^[57].

$$Y = e^{-(t/\delta)^p} \tag{47}$$

There are two parameters, δ (scale parameter, representing microbial resistance) and p (shape parameter, representing concavity) in the Weibull model^[49]. When $p < 1$, the shape is upwardly concave; when $p > 1$, downwardly concave, and for $p = 1$, a straight line on a log scale^[49]. The time t in the Weibull equation is sometimes replaced by a specific energy density.

The Weibull model has been tested by a number of studies, and has been remarkably successful in describing microbial inactivation kinetics, including in comparison to the Peleg and Hulsheger models^[54]. The presence of an extra parameter to describe the shape of the curve is an advantage. However, Peleg & Cole^[51] have posed the question of how the parameters may be derived from kinetic data. The question is whether the fitting of the model should be done as expressed in the form of Eqn 47, or whether to use the logarithmic form:

$$\ln(Y) = -\left(\frac{t}{\delta}\right)^p \tag{48}$$

In the presence of data scatter (which is typical of most microbiological data), the results from the two cases may be very different. Peleg & Cole^[51] note that when it is desired to accurately describe the behavior of the most resistant subpopulation of microorganisms, the logarithmic form of Eqn 46 should be used as the model.

Model comparisons

Various works have provided detailed summaries of kinetic models and their comparison. We present just a few here. Alvarenga et al.^[58], (compare first-order and Weibull models); Min et al.^[59] (first order, Peleg (Fermi) and Hulsheger models all gave satisfactory descriptions of inactivation); Saldaña et al.^[36] (Weibull model adequately described inactivation of *Salmonella typhimurium*); Donsi et al.^[60] and Pataro et al.^[61] (Weibull model adequately described inactivation of *Saccharomyces cerevisiae*); and Singh et al.^[62] (Hulsheger and Weibull models were superior to the Peleg and Bigelow (first-order or log-linear) models in describing inactivation of *Escherichia coli* in carrot juice).

Giner et al.^[63,64] determined kinetics of pectinesterase exposed to PEF (exponential decay pulses) in a batch chamber. The Weibull model yielded best accuracy over the Hulsheger, Fermi (Peleg) or first-order models. The advantage of this approach is the lack of residence time ambiguity, with the challenge being adequate separation of thermal vs. nonthermal effects.

For more details and comparisons, readers are referred to more comprehensive reviews such as Huang et al.^[49] who provide a detailed review of kinetic models and a large body of data on the same. They cover the four major tested models: first-order, Hulsheger, Peleg (Fermi) and Weibull, which have been compared in many studies, and two lesser-used models, the log-logistic^[65] and the Giner-Segui^[66] models. Also, Masood et al.^[67] review various models for emerging technologies, but are not solely focused on PEF.

Other models

Various other models have been considered in the literature, but have received less attention than the four discussed above.

Geeraerd et al.^[68] have developed the free software GINAFIT, which may be used to fit a wide variety of inactivation curves, some of which might have relevance to PEF. These are illustrated in Fig. 7.

Various models have been used to describe these curves.

Log linear model: This is essentially the same as the first-order model discussed earlier, and can only describe curves of shape I (Fig. 7a).

Log linear model with shouldering and/or tailing: This model enables the description of shapes I through IV, shown in Fig. 7a:

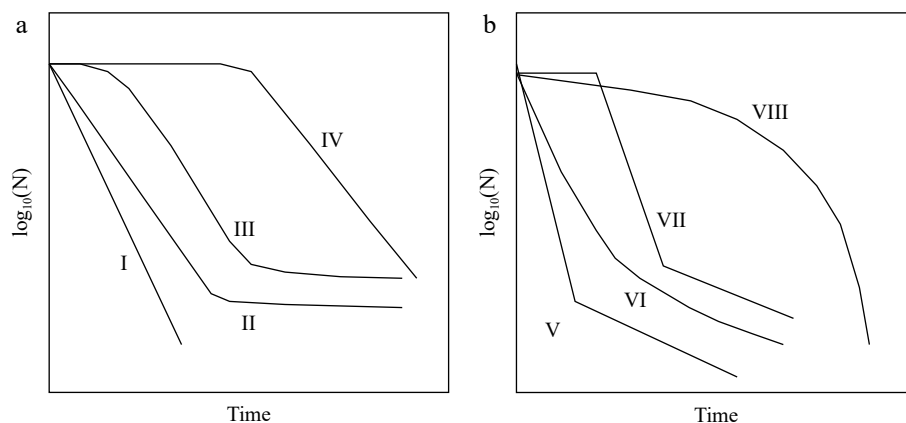


Fig. 7 Commonly observed survivor curves (after Geeraerd et al.^[68]). (a) I - linear; II - linear with tailing; III - sigmoidal; IV - linear with a preceding shoulder; (b) V - biphasic; VI - concave; VII - biphasic with shoulder; VIII - convex.

$$\left(\frac{N(t) - N_{res}}{N_0 - N_{res}}\right) = e^{-k_{max}t \left(\frac{e^{k_{max}S_1}}{1 + (e^{k_{max}S_1} - 1)e^{-k_{max}t}}\right)} \tag{49}$$

In this expression, two additional parameters are introduced: N_{res} , which represents the persistent residual population of microorganisms that remain following a typical nonthermal process (including a high pressure process); and S_1 , which denotes the duration of the 'shoulder' phase of Fig. 7 curves III and IV. Notably, when $S_1 = 0$ (i.e. no shoulder, equation 49 reduces to:

$$\left(\frac{N(t) - N_{res}}{N_0 - N_{res}}\right) = e^{-k_{max}t} \tag{50}$$

The Weibull model (Eqn 47) describes shapes I, VI and VII survivor curves from Fig. 7.

Biphasic models: These typically describe shapes I, II, V and VII in Fig. 7. Of particular interest in the two-fraction model of Cerf^[69]:

$$\log_{10}\left(\frac{N(t)}{N_0}\right) = f e^{-k_{max}t} + (1 - f)e^{-k_{max}2t} \tag{51}$$

where the population is composed of two sub-populations of different resistances.

Lebovka & Vorobiev^[70] attempted to provide a more mechanistic basis for the use of kinetic models. They noted that the first-order model is not applicable to describe PEF microbial inactivation data; the Hulsheger model, although popular, lacks theoretical justification; the Fermi log log and log logistic models are of an empirical nature. They investigated the Weibull model further, incorporating the effects of variable microbial and dimensions. A Gaussian distribution of cell diameters was assumed:

$$F(d_c) = \frac{1}{\sqrt{2\pi}\Delta} e^{-\left(\frac{d_c - \bar{d}_c}{2\Delta^2}\right)^2} \tag{52}$$

They then conducted a Monte Carlo simulation over a range of pore sizes and random orientations, and calculated the transient pore characteristic time (δ) for the Weibull model based on the relationship^[14] and using the relation of Schwan & Kay^[71] for the transmembrane potential. They were able to show that variation in cell diameters had a significant effect on the inactivation kinetic parameters. They also noted a number of simplifying assumptions in their model (no sublethal

damage, and variation in shapes) which need to be addressed further.

The Giner-Segui model^[49,66] is focused on enzyme inactivation during PEF, in particular, using the OSU-4F co-field treatment system, known to have significant hot zones^[38].

Timmermans et al.^[72] describe inactivation using the Gauss-Eyring model:

$$\log_{10}\left(\frac{N(t)}{N_0}\right) = \log_{10}\left(\frac{1}{2}\left[\operatorname{erfc}\left\{\frac{T - T_c(t)}{\sigma\sqrt{2}}\right\}\right]\right) \quad (53)$$

They used the model to describe inactivation of *Escherichia coli*, *Listeria monocytogenes*, *Lactobacillus plantarum*, *Salmonella* Senftenberg and *Saccharomyces cerevisiae* in orange juice.

Mendes-Oliveira et al.^[73] present a model which enables calculation of microbial inactivation as a function of energy density. The model is based on that of Peleg & Penchina^[74] modified to the form:

$$\frac{d\log S(\Delta E)}{d\Delta E} = -b(\Delta E)n(\Delta E)\left(-\frac{\log S(\Delta E)}{b(\Delta E)}\right)^{\frac{n(\Delta E)-1}{n(\Delta E)}} \quad (54)$$

where:

$$b(\Delta E) = \ln\left\{1 + e^{k(\Delta E - \Delta E_c)}\right\} \quad (55)$$

The model was successfully used to determine inactivation of *Escherichia coli* O157:H7 and *Salmonella* Typhimurium.

Li et al.^[30] presented an analytical solution for the transmembrane potential for a spherical cell exposed to a time-varying electric field. They used the analytical solution to the Laplace Eqn 27 which is a steady-state equation, but used time-varying boundary conditions. This (unlike Huang et al.^[23]) would tend to limit its accuracy to situations of sufficiently low frequency wherein the transient terms shown in Eqns 22 or 23 are not significant. Their solution showed that the highest transmembrane potentials occurred at the lowest frequencies, while at higher frequencies, the transmembrane potential decreased greatly. This suggests that low frequencies are more conducive to membrane damage than higher frequencies. Indeed, this is as expected based on experimental studies of Loghavi et al.^[75] which shows highest permeabilization at the lowest frequencies. Other works confirm this trend for eukaryotic cells^[13].

Guyot et al.^[76] hypothesize that yeast cell inactivation is at least partly thermal, and attempted to demonstrate it by (relatively) low field strength, long-duration PEF treatment of yeast cell suspensions. At the highest concentrations, significant increases in temperature rise were seen, suggesting that electroporation results in currents through yeast cells, resulting in their heating; the (relatively high electrical conductivity) exudate then increases temperature of the medium. This would appear to be an interesting challenge for future heat transfer modeling efforts.

Difficulties in determination of kinetics in flowing systems

A point of difficulty in determining kinetic parameters for PEF is the use of continuous flow equipment for the purpose. Early work^[25], since verified^[60] showed that continuous flow treatment resulted in greater PEF efficacy than static systems, the preference has been to conduct kinetic studies in continuous flow. Continuous flow devices result in residence time distributions, thus some uncertainty exists regarding the distribution of pulses received by different parts of the fluid (and the microorganisms contained therein) during passage through the

treatment chamber(s)^[77]. Thus, residence time uncertainties are overlaid on the probabilistic considerations regarding bacterial populations to make data analysis a formidable task. In addition, electric field inhomogeneities will add to this uncertainty. The problem becomes even more difficult when comparisons are made between different designs of treatment chambers, which represent entirely different flow regimes and dose distributions. When attempting to scale up from bench to pilot to plant scale, these variations may result in models that are unreliable on a larger scale.

Further, Valdramidis et al.^[78] make the important argument that nonlinear inactivation kinetics may be due to heterogeneous distribution of process conditions in the treatment chamber, which may mask the true inactivation kinetics. This is particularly true of PEF, where intense nonhomogeneities exist during processing. The authors further note that heat transfer within microbial clumps which has often been attributed to tailing has been shown to be of negligible significance due to extremely small sizes of clumps^[79]. Donsi et al.^[60] have also noted that even under static conditions, field heterogeneity resulted in increased survivors in the treatment chamber areas where field fringing effects resulted in a weakened electric field.

The resolution of these uncertainties is key to obtaining more reliable kinetic data. Towards this end, the approach is described by Delgado et al.^[80,81]. If the fractional retention can be modeled as an arbitrary scalar quantity using conservation equations (as, for example, Eqn 34), the rate of inactivation could be calculated while providing consideration of flow uncertainties.

In a notable variation on the common approach, Fox et al.^[82] describe PEF processing of *L. plantarum* in a microreactor wherein conditions may be carefully controlled. The actual device is described in an earlier paper^[83] by the authors.

The PEF microreactor consisted of two inline electrodes separated by a treatment section wherein the fluid was forced through a constriction causing intensification of the electric field therein. Fox et al.^[83] tested electroporation using vesicles containing carboxyfluorescein (CF) that has a concentration-dependent fluorescence intensity (at the high concentrations within the vesicles, the fluorescence intensity was low). When released into the solution by electroporation, the CF concentrations would drop, with stronger fluorescence, which was used as a measure of electroporation. Fox et al.^[82] successfully and noninvasively measured average temperature increase within the PEF unit post-pulsing by using Rhodamine B, a dye with fluorescence intensity which decreased with increasing temperature. Using this dye, it was confirmed that the microfluidic setup dissipated heat rapidly, resulting in a temperature increase of only 2.5 °C through the reactor.

The above setup enabled the authors to consider models which treat temperature and electric field effects separately^[82]. These were of the form of the first-order model (Eqn 37), with the reaction rate constant (k) being a function of temperature and electric field strength:

$$k = A\alpha(T)\beta(E) \quad (56)$$

where $\alpha(T)$ follows the Arrhenius relation:

$$\alpha(T) = e^{-\left(\frac{E_a}{RT}\right)} \quad (57)$$

For the electric field dependency, two different models were tested:

PEF modeling

$$\beta(E) = (E - E_{crit}) \quad (58)$$

and:

$$\beta(E) = e^{-\left(\frac{E_{act}}{E}\right)^2} \quad (59)$$

Both models were found to be good descriptors of the inactivation kinetics. Notably, an unexpectedly high value of E_{crit} (critical electric field strength above which inactivation is zero) was found, which was attributed to the extremely resistant nature of the strain of *L. plantarum*.

We note that the authors have used the theories of the field strength required for electroporation^[2,10,14,84] in their assumptions about critical field strength. It is worth noting that since that time, it has been shown that even relatively small fields can cause permeabilization and inactivation^[85,86], so the older theories of Abidor, Weaver and Schwan may need to be revisited.

Overall summary

We have presented three broad categories of modeling for PEF systems; consideration of electroporation, which is ultimately a molecular-level process, requiring modeling tools such as molecular dynamics; treatment chamber or pilot scale models, which involve continuum mechanics based models, and finally kinetic models that are useful for designing processes, but which must be combined with treatment chamber scale models to design PEF processes. Much still remains to be done, since PEF processes are intense, fleeting, and difficult to measure by experimental techniques. All symbols and Greek letters appearing in the text and equations are listed in [Supplemental File 1](#).

Acknowledgments

Financial and research support provided by the College of Food, Agricultural and Environmental Sciences, The Ohio State University, via USDA Multistate Research Project NC-1023, *Engineering for Food Safety and Quality*. References to commercial products or trade names are made with the understanding that no endorsement or discrimination by The Ohio State University is implied.

Conflict of interest

The author declares that there is no conflict of interest.

Supplementary Information accompanies this paper at (<https://www.maxpress.com/article/doi/10.48130/FIA-2023-0012>)

Dates

Received 6 March 2023; Accepted 17 April 2023; Published online 5 July 2023

References

- Sale AJH, Hamilton WA. 1967. Effects of high electric fields on microorganisms. I. Killing of bacteria and yeasts. *Biochimica et Biophysica Acta (BBA) - General Subjects* 148:781–88
- Hamilton WA, Sale AJH. 1967. Effects of high electric fields on microorganisms. II. Mechanism of action of the lethal effect. *Biochimica et Biophysica Acta (BBA) - General Subjects* 148:789–800
- Collin A, Bruhier, H Kolosnjaj J, Golzio M, Rols MP, et al. 2022. Spatial mechanistic modeling for prediction of 3D multicellular spheroids behavior upon exposure to high intensity pulsed electric fields. *AIMS Bioengineering* 9(2):102–22
- Peng Y, Liao Z, Zhang Y, Fang Y, Qiu Z, et al. 2022. Analysis of deformation dynamics of droplet in oil under the CPG electric field. *Chemical Engineering Research and Design* 183:357–67
- Sato T, Murakami Y, Muramoto Y. 2019. Estimation of liquid sterilization using critical voltage under high electric field pulses. *IEEE Transactions on Electrical and Electronic Engineering* 14:1002–7
- International Commission on Microbiological Specifications for Foods (ICMSF). 2006. A simplified guide to understanding and using food safety objectives and performance objectives. www.icmsf.org/wp-content/uploads/2018/02/GuiaSimplificado-English.pdf
- Siemer C. 2022. Improved Pulsed Electric Field processing units for decontamination of thermosensitive protein-rich foods. *Presentation no. OR-117, the 4th World Congress on Electroporation, Copenhagen, Denmark, October 9–13, 2022*. <https://wc2022.electroporation.net/event/program/#track-533>
- Michael DH, O'Neill ME. 1970. Electrohydrodynamic instability in plane layers of fluid. *Journal of Fluid Mechanics* 41:571–80
- Crowley JM. 1973. Electrical breakdown of bimolecular lipid membranes as an electromechanical instability. *Biophysical Journal* 13:711–24
- Abidor IG, Arakelyan VB, Chernomordik LV, Chizmadzhev YA, Pastushenko VF, et al. 1979. Electric breakdown of bilayer lipid membranes I. The main experimental facts and their qualitative discussion. *Bioelectrochemistry and Bioenergetics* 6:37–52
- Pastushenko VF, Chizmadzhev YA, Arakelyan VB. 1979. Electric breakdown of bilayer lipid membranes II. Calculation of the membrane lifetime in the steady-state diffusion approximation. *Bioelectrochemistry and Bioenergetics* 6:53–62
- Cho HY, Yousef AE, Sastry SK. 1996. Growth kinetics of *Lactobacillus acidophilus* under ohmic heating. *Biotechnology and Bioengineering* 49:334–40
- Kulshrestha SA, Sastry SK. 2003. Frequency and voltage effects on enhanced diffusion during Moderate Electric Field (MEF) treatment. *Innovative Food Science & Emerging Technologies* 4(2):189–94
- Weaver JC, Chizmadzhev YA. 1996. Theory of electroporation: a review. *Bioelectrochemistry and Bioenergetics* 41:135–60
- Parseghian A. 1969. Energy of an ion crossing a low dielectric membrane: solutions to four relevant electrostatic problems. *Nature* 221:844–46
- Shillcock JC, Seifert U. 1998. Thermally induced proliferation of pores in a model fluid membrane. *Biophysical Journal* 74:1754–66
- Neu JC, Krassowska W. 1999. Asymptotic model of electroporation. *Physical Review E* 59(1):3471–82
- Smith, KC. 2006. *Modeling cell and tissue electroporation*. M. S. Thesis, Massachusetts Institute of Technology, Cambridge, MA.
- Mukhopadhyay P, Vogel HJ, Tieleman DP. 2004. Distribution of Pentachlorophenol in phospholipid bilayers: A molecular dynamics study. *Biophysical Journal* 86(1):337–45
- Vernier PT, Ziegler MJ. 2007. Nanosecond field alignment of head group and water dipoles in electroporating phospholipid bilayers. *The Journal of Physical Chemistry* 111:12993–96
- Böckmann RA, de Groot BL, Kakorin S, Neumann E, Grubmüller H. 2008. Kinetics, statistics and energetics of lipid membrane electroporation studied by molecular dynamics simulations. *Biophysical Journal* 95:1837–50
- Griese T, Kakorin S, Neumann E. 2002. Conductometric and electrooptic relaxation spectrometry of lipid vesicle electroporation at high fields. *Physical Chemistry Chemical Physics* 4:1217–27

23. Huang K, Jiang T, Wang, W, Gai L, Wang J. 2014. A comparison of pulsed electric field resistance for three microorganisms with different biological factors in grape juice via numerical simulation. *Food and Bioprocess Technology* 7:1981–95
24. Yin Y, Zhang QH, Sastry SK. 1997. High voltage pulsed electric field treatment chambers for the preservation of liquid food products. *USA, Patent* 5, 690, 978.
25. Martín O, Qin BL, Chang FJ, Barbosa-Cánovas GV, Swanson BG. 1997. Inactivation of *Escherichia coli* in skim milk by high intensity pulsed electric fields. *Journal of Food Process Engineering* 20:317–36
26. Toepfl S, Heinz V, Knorr D. 2007. High intensity pulsed electric fields applied for food preservation. *Chemical Engineering and Processing: Process Intensification* 46(6):537–46
27. Qin B, Zhang Q, Barbosa-Cánovas GV, Swanson BG, Pedrow PD. 1995. Pulsed electric field treatment chamber design for liquid food pasteurization using a finite element method. *Transactions of the ASAE* 38:557–65
28. Misaki T, Tsuboi H, Itaka K, Hara T. 1982. Computation of three-dimensional electric field problems by a surface charge method and its application to optimum insulator design. *IEEE Transactions on Power Apparatus and Systems PAS* PAS-101:627–34
29. Góngora-Nieto MM, Pedrow PD, Swanson BG, Barbosa-Cánovas GV. 2003. Impact of air bubbles in a dielectric liquid when subject to high field strengths. *Innovative Food Science & Emerging Technology* 4:57–67
30. Li J, Wei X, Wang Y, Liu G. 2009. Analysis for relationship of transmembrane potential-pulsed electric field frequency. *Food and Bioprocess Technology* 87:261–65
31. Fiala A, Wouters PC, van den Bosch E, Creyghton YLM. 2001. Coupled electrical-fluid model of pulsed electric field treatment in a model food system. *Innovative Food Science and Emerging Technology* 2:229–38
32. Gerlach D, Alleborn N, Baars A, Delgado A, Moritz J, et al. 2008. Numerical simulations of pulsed electric fields for food preservation: a review. *Innovative Food Science and Emerging Technologies*, 9:408–17
33. Jaeger H, Meneses N, Knorr D. 2009. Impact of PEF treatment inhomogeneity such as electric field distribution, flow characteristics and temperature effects on the inactivation of *E. coli* and milk alkaline phosphatase. *Innovative Food Science and Emerging Technologies* 10:470–80
34. Buckow R, Schroeder S, Berres P, Baumann P, Knoerzer K. 2010. Simulation and evaluation of pilot-scale pulsed electric field (PEF) processing. *Journal of Food Engineering* 101:67–77
35. Meneses N, Jaeger H, Knorr D. 2011. Minimization of thermal impact by application of electrode cooling in a co-linear PEF treatment chamber. *Journal of Food Science* 76(8):E536–E543
36. Saldaña G, Puértolas E, Álvarez I, Meneses N, Knorr D, et al. 2010. Evaluation of a static treatment chamber to investigate kinetics of microbial inactivation by pulsed electric fields at different temperatures at quasi-isothermal conditions. *Journal of Food Engineering* 100:349–56
37. Delgado A, Kulisiewicz L, Rauh C, Wierschem A. 2012. Fluid dynamics in novel thermal and non-thermal processes. In *Novel Thermal and Non-Thermal Technologies for Fluid Foods*, eds. Cullen PJ, Tiwari BK, Valdramidis VP. Academic Press, Elsevier. pp.7–33. <https://doi.org/10.1016/B978-0-12-381470-8.00002-5>
38. Salengke S, Sastry SK, Zhang QH. 2012. Pulsed electric field technology: modeling of electric field and temperature distributions within continuous flow PEF treatment chamber. *International Food Research Journal* 19(3):1137–44
39. Pataro G, Barca GMJ, Donsi G, Ferrari G. 2015. On the modeling of electrochemical phenomena at the electrode-solution interface in a PEF treatment chamber: Methodological approach to describe the phenomenon of metal release. *Journal of Food Engineering* 165:34–44
40. Pataro G, Barca GMJ, Donsi G, Ferrari G. 2015. On the modelling of the electrochemical phenomena at the electrode-solution interface in a PEF treatment chamber: Effect of electrical parameters and chemical composition of model liquid food. *Journal of Food Engineering* 165:45–51
41. Krauss J, Ertunç Ö, Rauh C, Delgado A. 2011. Novel, multi-objective optimization of pulsed electric field (PEF) treatment for liquid food treatment. In *Multiphysics Simulation of Emerging Food Processing Technologies*, eds. Knoerzer K, Juliano P, Roupas P, Versteeg C. John Wiley & Sons. 374 pp.
42. Lindgren M, Aronsson K, Galt S, Ohlsson T. 2002. Simulation of the temperature increase in pulsed electric field (PEF) continuous flow treatment chambers. *Innovative Food Science & Emerging Technologies* 3(3):233–45
43. Rauh C, Baars A, Delgado A. 2009. Uniformity of enzyme inactivation in a short-time high-pressure process. *Journal of Food Engineering* 91:154–63
44. Jaeger H, Meneses N, Moritz J, Knorr D. 2010. Model for the differentiation of temperature and electric field effects during thermal assisted PEF processing. *Journal of Food Engineering* 100:109–18
45. Buckow R, Semrau J, Sui Q, Wan J, Knoerzer K. 2012. Numerical evaluation of lactoperoxidase inactivation during continuous pulsed electric field processing. *Biotechnology Progress* 28(5):1363–75
46. Duvoisin CA, Horst DJ, Vieira RA, Baretta D, Pscheidt A, et al. 2022. Finite element simulation and practical tests on Pulsed Electric Field (PEF) for packaged food pasteurization: inactivating *E. coli*, *C. difficile*, *Salmonella spp.* and mesophilic bacteria. *Food Science and Technology* 42:e115421
47. Ganea I. 2017. Influence of the solid dielectric over the electric field from the ozone cell gap with double dielectric barrier. *IOP Conference Series: Materials Science and Engineering* 200:012058
48. Raso J, Alvarez I, Condón S, Sala Trepat FJ. 2000. Predicting inactivation of *Salmonella senftenberg* by pulsed electric fields. *Innovative Food Science and Emerging Technologies* 1:21–29
49. Huang K, Tian H, Gai L, Wang J. 2012. A review of kinetic models for inactivating microorganisms and enzymes by pulsed electric field processing. *Journal of Food Engineering* 111:191–207
50. Sensoy I, Zhang QH, Sastry SK. 1997. Inactivation kinetics of *Salmonella dublin* by Pulsed Electric Field. *Journal of Food Process Engineering* 20(5):367–81
51. Peleg M, Cole MB. 1998. Reinterpretation of microbial survival curves. *Critical Reviews in Food Science and Nutrition* 38(5):353–80
52. Hülshager H, Potel J, Niemann EG. 1981. Killing of bacteria with electric pulses of high field strength. *Radiation and Environmental Biophysics* 20(1):53–65
53. Sale AJH, Hamilton WA. 1968. Effects of high electric fields on micro-organisms: III. Lysis of erythrocytes and protoplasts. *Biochimica et Biophysica Acta (BBA) – Biomembranes* 163(1):37–43
54. San Martín MF, Sepúlveda DR, Altunakar B, Góngora-Nieto MM, Swanson BG, et al. 2007. Evaluation of selected mathematical models to predict the inactivation of *Listeria innocua* by pulsed electric fields. *LWT – Food Science and Technology* 40(7):1271–79
55. Peleg M. 1995. A model of microbial survival after exposure to pulsed electric fields. *Journal of the Science of Food and Agriculture* 67(1):93–99
56. Zhong K, Chen F, Wang Z, Wu J, Liao X, et al. 2005. Inactivation and kinetic model for the *Escherichia coli* treated by a co-axial pulsed electric field. *European Food Research and Technology* 221(6):752–58
57. Mafart P, Couvert O, Gaillard S, Leguerinel I. 2002. On calculating sterility in thermal preservation methods: application of the Weibull frequency distribution model. *International Journal of Food Microbiology* 72:107–13

PEF modeling

58. Alvarenga VO, Brito LM, Lacerda ICA. 2022. Application of mathematical models to validate emerging processing technologies in food. *Current Opinion in Food Science* 48:100928
59. Min S, Min SK, Zhang QH. 2003. Inactivation kinetics of tomato juice lipoxygenase by pulsed electric fields. *Journal of Food Science* 68(6):1995–2001
60. Donsi G, Ferrari G, Pataro G. 2007. Inactivation kinetics of *Saccharomyces cerevisiae* by pulsed electric fields in a batch treatment chamber: The effect of electric field unevenness and initial cell concentration. *Journal of Food Engineering* 78:784–92
61. Pataro G, Senatore B, Donsi G, Ferrari G. 2011. Effect of electric and flow parameters on PEF treatment efficiency. *Journal of Food Engineering* 105:79–88
62. Singh J, Singh M, Singh B, Nayak M, Ghanshyam C. 2017. Comparative analyses of prediction models for inactivation of *Escherichia coli* in carrot juice by means of pulsed electric fields. *Journal of Food Science and Technology* 54(6):1538–44
63. Giner J, Grouberman P, Gimeno V, Martín O. 2005. Reduction of pectinesterase activity in a commercial enzyme preparation by pulsed electric fields: comparison of inactivation kinetic models. *Journal of the Science of Food and Agriculture* 85:1613–21
64. Giner J, Bailo E, Gimeno V, Martín-Belloso O. 2005. Models in a Bayesian framework for inactivation of pectinesterase in a commercial enzyme formulation by pulsed electric fields. *European Food Research and Technology* 221:255–64
65. Cole MB, Davies KW, Munro G, Holyoak CD, Kilsby DC. 1993. A vitalistic model to describe the thermal inactivation of *Listeria monocytogenes*. *Journal of Industrial Microbiology* 12:232–39
66. Giner-Seguí J, Bailo-Ballarín E, Gorinstein S, Martín-Belloso O. 2006. New kinetic approach to the evolution of polygalacturonase (EC 32.2.1.15) activity in a commercial enzyme preparation under pulsed electric fields. *Journal of Food Science* 71(6):E262–E269
67. Masood H, Trujillo FJ, Knoerzer K, Juliano P. 2018. Designing, Modeling, and Optimizing Processes to Ensure Microbial Safety and Stability Through Emerging Technologies. In *Innovative Technologies for Food Preservation*, eds. Barba FJ, Sant'Ana AS, Orlén V, Koubaa M. Academic Press. pp. 187–229. <https://doi.org/10.1016/B978-0-12-811031-7.00006-6>
68. Geeraerd AH, Valdramidis VP, Van Impe JF. 2005. GlnaFIT, a free-ware tool to assess non-log-linear microbial survivor curves. *International Journal of Food Microbiology* 102:95–105
69. Cerf O. 1976. A review: Tailing of survival curves of bacterial spores. *Journal of Applied Bacteriology* 42:1–19
70. Lebovka NI, Vorobiev E. 2004. On the origin of the deviation from the first-order kinetics in inactivation of microbial cells by pulsed electric fields. *International Journal of Food Microbiology* 91:83–89
71. Schwan HP, Kay CF. 1957. The conductivity of living tissues. *Annals of the New York Academy of Sciences* 65(6):1007–13
72. Timmermans RAH, Mastwijk HC, Berendsen LBJM, Nederhoff AL, Matser AM et al. 2019. Moderate intensity pulsed electric fields (PEF) as alternative mild preservation technology for fruit juice. *International Journal of Food Microbiology* 298:63–73
73. Mendes-Oliveira G, Jin TZ, Campanella OH. 2020. Modeling the inactivation of *Escherichia coli* O157:H7 and *Salmonella* Typhimurium in juices by pulsed electric fields: The role of the energy density. *Journal of Food Engineering*, 282:110001
74. Peleg M, Penchina CM. 2000. Modeling Microbial Survival during Exposure to a Lethal Agent with Varying Intensity. *Critical Reviews in Food Science and Nutrition* 40(2):159–72
75. Loghavi L, Sastry SK, Yousef AE. 2009. Effect of moderate electric field frequency and growth stage on the cell membrane permeability of *Lactobacillus acidophilus*. *Biotechnology Progress* 25(1):85–94
76. Guyot S, Ferret E, Boehm JB, Gervais P. 2007. Yeast cell inactivation related to local heating induced by low-intensity electric fields with long-duration pulses. *International Journal of Food Microbiology* 113:180–88
77. Sastry SK. 2016. Toward a philosophy and theory of volumetric nonthermal processing. *Journal of Food Science* 81(6):E1431–E1446
78. Valdramidis VP, Taoukis PS, Stoforos NG, and Van Impe, JFM. 2012. Modeling the kinetics of microbial and quality attributes of fluid food during novel thermal and non-thermal processes. In *Novel Thermal and Non-Thermal Technologies for Fluid Foods*, eds. Cullen PJ, Tiwari BK, Valdramidis VP. Academic Press, Elsevier. pp. 433–71. <https://doi.org/10.1016/B978-0-12-381470-8.00014-1>
79. Hasting APM, Blackburn CDW, Crowther JS. 2001. *Mycobacterium paratuberculosis* and the commercial pasteurization of milk. *Food and Bioprocess Processing* 79:83–88
80. Delgado A, Rauh, C, Kowalczyk W, Baars A. 2008. Review of modelling and simulation of high-pressure treatment of materials of biological origin. *Trends in Food Science & Technology* 19:329–36
81. Delgado A, Hartmann C. 2003. *Pressure treatment of food: instantaneous but not homogeneous effect*. In *Advances in High Pressure Bioscience and Biotechnology II*, ed. Winter R. Berlin, Heidelberg: Springer, Heidelberg. pp. 459–64. https://doi.org/10.1007/978-3-662-05613-4_83
82. Fox MB, Esveld DC, Mastwijk H, Boom RM. 2008. Inactivation of *L. plantarum* in a PEF microreactor: the effect of pulse width and temperature on the inactivation. *Innovative Food Science and Emerging Technologies* 9:101–8
83. Fox MB, Esveld E, Luttge R, Boom R. 2005. A new pulsed electric field microreactor: Comparison between the laboratory and microscale. *Lab on a Chip* 5(9):943–48
84. Kinoshita K Jr, Ashikawa I, Saita N, Yoshimura H, Itoh H, et al. 1988. Electroporation of cell membrane visualized under a pulsed-laser fluorescence microscope. *Biophysical Journal* 53,(1988):1015–19
85. Loghavi L, Sastry SK, Yousef AE. 2007. Effect of Moderate Electric Field on the metabolic activity and growth kinetics of *Lactobacillus acidophilus*. *Biotechnology and Bioengineering* 98(4):872–81
86. Mok JH, Pyatkovskyy T, Yousef AE, Sastry SK. 2019. Combined effect of shear stress and moderate electric field on the inactivation of *Escherichia coli* K12 in apple juice. *Journal of Food Engineering* 262:121–30



Copyright: © 2023 by the author(s). Published by Maximum Academic Press on behalf of China Agricultural University, Zhejiang University and Shenyang Agricultural University. This article is an open access article distributed under Creative Commons Attribution License (CC BY 4.0), visit <https://creativecommons.org/licenses/by/4.0/>.